Effect of welding speed on the mechanical properties and weld defects of 7075 Al alloy joined by FSW

B. Çevik[1]*, Y. Özçatalbaş[2], B. Gülenç[2]

[1]*Düzce University, Department of Welding Technology, 81850 Düzce, Turkey*
[2]*Gazi University, Department of Metallurgy & Materials Engineering, 06500 Ankara, Turkey*

Abstract

In this study, 7075-T651 Al alloys were joined by friction stir welding (FSW) at a fixed rotational speed and different welding speeds. The stirring tool used in the welding processes was comprised of a shoulder of 20 mm in diameter and modified M6 × 1 HSS hand taps used as pins. The FSW was performed at a rotational speed of 1600 rpm and at welding speeds of 20, 40, and 60 mm min^{-1}. Mechanical and metallographic tests were carried out on the welded joints and the effects of the welding speed on the mechanical and metallurgical properties of the welded specimens were investigated. Welding speed significantly affected the microstructure and mechanical properties of the joining. Results showed that the average grain size of the weld nugget was reduced as welding speed was increased. In addition, it was found that high welding speed negatively affected the mechanical properties of the weld nugget.

K e y   w o r d s: FSW, aluminium alloy, mechanical properties, micro defects, microstructure

1. Introduction

The 7075 Al alloys become hardened through precipitation. They are commonly used in the aviation and defence industries due to their highly desirable characteristics of lightness, high strength, corrosion resistance and forming capabilities. The highest mechanical properties of 7075 Al alloy are achieved through T6/T651 heat treatment [1–3].

Friction stir welding (FSW) is a solid-state joining technique for butt and lap welding of ferrous and non–ferrous metals invented and patented in 1991 by The Welding Institute (TWI) [4, 5]. Due to its unique advantages, including short weld time, minimum surface preparation and ease of automation, FSW is an alternative technique to arc welding for the joining of same or different materials having difficult welding capabilities [4, 6]. Friction stir welding demonstrates an especially successful performance in the joining of aluminium alloys which are difficult to weld using traditional welding methods. The technique can even be used effectively on 2xxx and 7xxx Al alloys, in particular on alloy 7075 [4]. The fractures that appear in the welding of Al alloys are caused by the wide solidifica-

tion temperature range of these alloys and their high thermal expansion coefficients. The high heat input in arc welding causes fractures in aluminium alloys. This results from their high thermal expansion and a wide range of solidification temperatures, especially when precipitation hardening is applied to the welding seams [4, 7]. The 7xxx series aluminium alloys have a high cracking sensitivity based on the rate of Cu in their composition. A very limited number of 7xxx series aluminium alloys can be welded. Due to its high Cu content, 7075 Al alloy is among these, but because of its poor welding capability, using traditional welding methods is not recommended [4–8]. Consequently, there have been a number of studies conducted on the weldability of the 7xxx series Al alloys. In these investigations, the shoulder and pin design and welding parameters were taken into account [2, 3, 5–7, 9, 10]. Gemme et al. [9] and Akbarinia et al. [10] reported that one of the most effective parameters affecting the mechanical response and microstructural features was welding speed. Welding optimization and various stirring tool geometries have also been considered in the search for effective factors on mechanical behaviour and microstructure. There have been a number of

*Corresponding author: tel.: +90 380 7314005; fax: +90 380 7313124; e-mail address: bekircevik@duzce.edu.tr

T a b l e 1. Mechanical properties of 7075–T651 Al alloy

Yield stress σ_a (MPa)	Tensile stress σ_c (MPa)	% Elongation	Elasticity module (GPa)	Hardness, HR_B
545.1	610.5	12	72	90

studies in the literature which have been conducted on the joining of Al and its alloys by FSW. Moreover, studies investigating the complex microstructural aspects and microstructure defects of materials joined by the FSW process continue to be carried out [4–7, 9–16].

In this study, 7075-T651 Al alloy specimens were joined by FSW at a fixed rotational speed and different welding speeds. Tensile and hardness tests and metallographic examinations were performed on the completed weld joints, and the effect of welding speed on the mechanical and microstructure characteristics of the joining zone was examined.

2. Experimental procedure

2.1. Material

In this study, specimens having the dimensions of $6 \times 125 \times 300\,\mathrm{mm}^3$ were prepared from 7075-T651 Al alloy (5.1–6.1 % Zn, 2.1–2.9 % Mg, 1.2–2 % Cu, 0.18–0.28 % Cr, ≤ 0.30 % Mn). Table 1 lists the mechanical properties of this alloy.

2.2. Method

A tool with an adjustable pin size was produced to be used in the welding process. This tool consisted of two parts: shoulder and pin. The shoulder, with a diameter of 20 mm, was made of X210Cr12 steel while the pins were produced using M6 × 1 HSS hand taps modified to an angle of 2°. Pin height was adjusted to 5.8 mm. Figure 1 shows details of the pin geometry and size.

Welding processes were performed with a FIRST MCV 300 CNC milling machine. Before joining, the Al plates were fixed on another plate of the same type. The shoulder was immersed at a constant 0.2 mm depth. Thus, the axial load was kept constant for all specimens. Welding was performed at a constant rotational speed of 1600 rpm with welding speeds of 20, 40, and 60 mm min^{-1}. After welding, the thickness of the welded sample was trimmed to 2.5 mm in order to prevent the tunnelling effect. Also, reference metal (N-Ref.) was trimmed to 2.5 mm in order to be in the same geometrical dimensions. All mechanical tests were performed on these specimen dimensions. Specimens were coded as "Nrpm-welding speed": N1600-20, N1600-40, N1600-60. In addition to
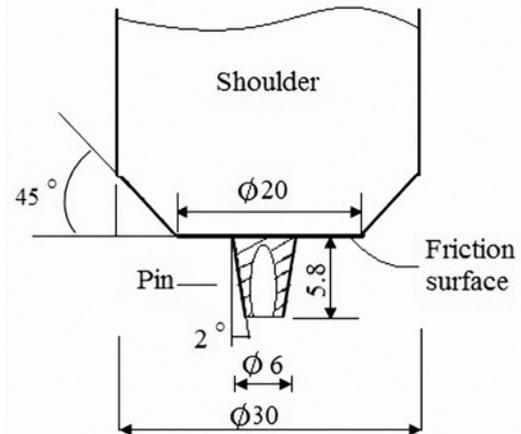
Fig. 1. Shoulder and pin in joining process.

metallographic tests, the welded specimens were subjected to mechanical tests which included tensile and hardness tests. For the metallographic examination, specimens taken from the cross-section perpendicular to the welding direction were prepared by etching with Keller's reagent (190 ml distilled water, 5 ml HNO$_3$, 3 ml HCl, 2 ml HF) for 90–120 s. Tensile specimens were prepared in accordance with ASTM-E8. Macrostructural examinations of the specimens were performed using a Dino-Lite (Pro) Digital Microscope; a Leica DM 4000M metal microscope was used for the microstructural examinations. The average grain size of the weld metal was determined via mean linear intercept (MLI). Microvoids and large grain band zones were examined using a JEOL JSM-6060LV Scanning Electron Microscope (SEM). Hardness measurements were carried out by applying a load of 100 kgf for 10 s with a steel ball of 1/16" in a universal hardness test device. Tensile tests were performed at a speed of 10 mm min^{-1} employing a universal tensile test device.

3. Results and discussion

3.1. Macrostructural analysis

All specimens were joined with a margin of error up to the diameter of the stirring tool at the starting and ending points. When the surface images of the welded plates were examined, no macro-scale surface
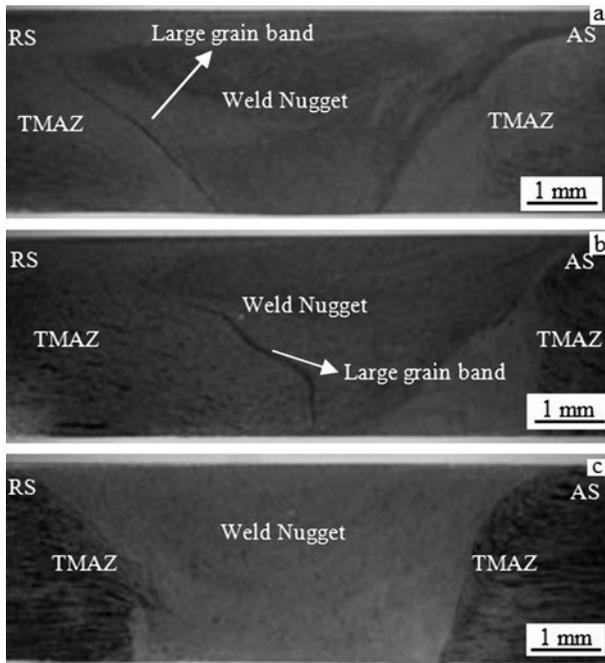
Fig. 2. Macrostructure images of specimens joined by FSW: a) N16000-20, b) N1600-40, and c) N1600-60.

defects were detected on the weld nuggets; however, burrs and corrugation were observed on the retreating side (RS) of the weld nuggets. These corrugations were the result of the plasticization of the Al alloy caused by frictional heat from the movement of the shoulder retreating in the rotational direction [4].

Tunnel defects appeared in the root portion along the length of the weld nugget in all specimens. These were thought to be caused by the applied welding speed. An increased welding speed reduced the heat input to the welding zone [4, 11, 12]. As a result, the heat generated in the root portion of the weld nugget was not sufficient. This insufficient heating of the root part of the weld nugget could have been caused by failure to create a thermodynamic balance between the heat input applied during the welding process and the heat transfer rate of the joined materials [13, 16, 17]. It was assumed that the tunnel defects had formed due to the insufficient plasticization of the combined materials in this zone, which was exposed to low heat input.

Figure 2 shows macrostructure images of the specimens joined through FSW. Zones involving the weld nugget and the thermo-mechanically affected zone (TMAZ) did not have symmetrical characteristics. Different macrostructural characteristics were created on the advancing side (AS) and retreating side (RS) of the TMAZs, depending on the rotational direction of the stirring tool during welding. The grains on the AS were directed to the surface by the friction of the shoulder during stirring. Although the weld nugget

TMAZ borders on the AS were clearly formed, their development was not evident on the RS. The upper surfaces of the plates were exposed to high heat input because of the friction of the tool. Therefore, the weld nugget expanded towards the upper surface of the plates. Large grain bands were observed on the retreating sides of the N1600-20 and N1600-40 specimens (Figs. 2a,b).

3.2. Microstructural analysis

The microstructure image of the 7075-651 Al alloy exhibited the deformation texture of the structures (grains) which were formed in the aluminium plate during the cold rolling process.

During the FSW, a high level of plastic deformation occurred, especially on the weld nugget. The grains with a low aspect ratio in the metal base structure were fragmented and transformed into smaller coaxial grains. This was attributed to the high temperature and plastic deformation at high rotational speed. Furthermore, as a result of the high temperature, the grain structure of the weld nuggets of all specimens were recrystallized and stirred homogeneously, resulting in deformation. The findings showed that the average grain size became smaller as welding speed increased. The average grain size of the N1600-20 sample was 5.7 μm and for the N1600-60 sample it was 4.5 μm. This was ascribed to the fact that, as the welding speed increased, the frictional heat formed at the welding zone decreased.

Figure 3 illustrates the microstructure defects on the weld nuggets. Large grain bands could be seen on the RS in the weld nuggets of the N1600-20 and N1600-40 specimens. There were many examples of weakly joined areas. In the literature, such structures are referred to as "kissing bonds" and may be found close to the root portions and transition zones of the weld nuggets. Additionally, such defects can always be seen to follow the welding bond line. The formation of such zones was assumed to be caused by the weak plasticization of the metal joined by increased welding speed [18, 19]. These zones were characterized by a darker colour as a result of the etching with Keller's reagent (Figs. 2a,b). The SEM examination of these zones showed microvoids appearing in a line. Grain coarsening occurred around this microvoid line. Presumably, the microvoid defects reduced the heat transfer and resulted in the large grains seen in the microstructure (Figs. 3a,b). Unlike the other specimens, in N1600-60, a porous structure was formed in the root portion of the RS of the weld nugget zones which had not been homogeneously stirred (Fig. 3c).

3.3. EDS analysis

The scanning electron microscopy-energy disper-
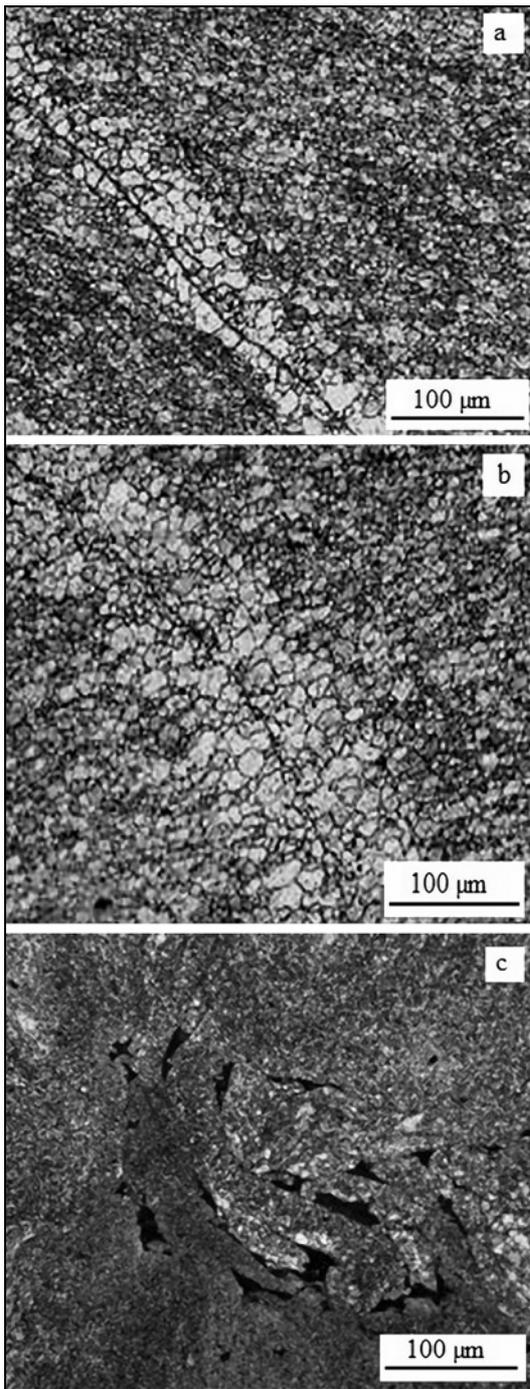
Fig. 3. Microstructural defects: a) large grain bands in N1600-20, b) large grain bands in N1600-40, and c) microstructure of root portion of N1600-60.

Fig. 4. Specimen N1600-40: a) SEM image, b) EDS analysis points.

sive spectroscopy (SEM-EDS) examination was performed on the N1600-40 specimen in order to further analyse the zones with microstructural defects (Fig. 4). Some researchers [20–22] have stated that the formation of such zones was caused by the aggregation of oxide inclusions, or by some precipitation phases in them under the effect of the vortex movement created

by the rotation of the stirring tool. An EDS point analysis was done in order to determine the chemical composition of this zone. The analysis showed that the chemical composition of the measured points had similar characteristics (Fig. 5).

In order to identify the types of defects on the images, back-scattered SEM pictures were taken from the unetched surface only. When the image of specimen N1600-40 was analysed, no crack defects were observed (Fig. 6). However, microvoids of a minimum size of 2 μm and a maximum size of 5 μm were detected on the RS of the weld nugget. These void defects that formed on the RS were attributed to an insufficient amount of material having been transferred from the pin side during the stirring. The structure seen as a continuous band on the retreating side is actually the large grain area, having a width of approximately 100 μm and composed of large grains with an average size of 6 μm (Fig. 3b). The grain coarsening that appeared in these areas was thought to be a result of the microvoids acting as a barrier preventing
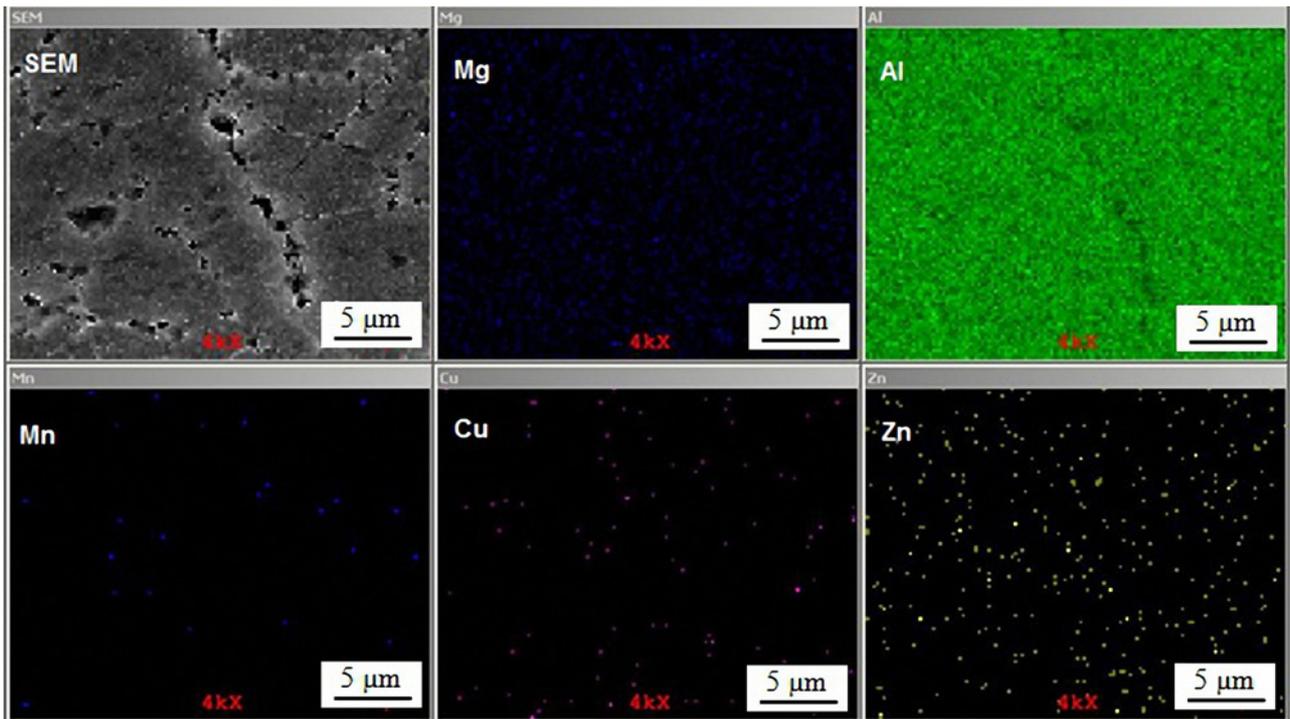
Fig. 5. Elemental map of the area of specimen N1600-40 analysed by EDS.
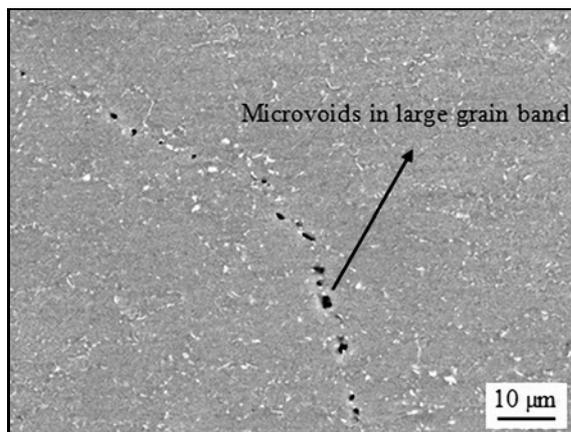
Fig. 6. SEM (back-scatter) image of the unetched surface of specimen N1600-40.

Fig. 7. Hardness distribution of welded regions N1600-40.

the transmission of heat. Grains outside of this area had an average size of 5.2 μm.

3.4. Hardness test results

Figure 7 shows the hardness distributions of the welded specimens. The hardness values of the weld centres of specimens N1600-20, N1600-40, and N1600-60 were measured, respectively, as 70.6 HR$_B$, 73.6 HR$_B$, and 76.9 HR$_B$. When the graphics were analysed, it was generally observed that the hardness values of the weld zone increased with the increasing

welding speed. Low hardness values were observed in zones close to the shoulder width (the TMAZs). In addition, with the increase in welding speed, between the TMAZs and the weld centre the distances of the points of measured minimum hardness values were reduced. A W-shaped hardness distribution was formed in all specimens. The W-shaped hardness distribution is a typical characteristics of precipitation hardening alloys joined with FSW [3, 18]. Hardness and strength increase when T6/T651 heat treatment is applied in the production phase of 7075 Al alloys [2]. Moreover, as an effect of deformation, the fine precipitates of

T a b l e 2. Mechanical properties of welded specimens

Specimen code	Tensile stress (MPa)	% Elongation	Weld efficiency (%)
N-Ref.	610.5	12	–
N1600-20	363.2	4.3	60
N1600-40	389	4.8	64
N1600-60	370.2	2.7	61

the Guinier-Preston (GP) zones are dissolved when the weld zone is heated up locally to 450 °C. Other researchers have also stated that hardener ($MgZn_2$) precipitates in 7075 Al alloys were dissolved and then transformed into precipitates with fewer hardening characteristics [2, 18, 19].

3.5. Tensile test results

Table 2 illustrates the mechanical properties of the welded specimens produced at 1600 rpm. As a result of tensile tests performed on the N–Reference specimen, the maximum tensile strength was found to be 610.5 MPa, whereas the elongation (breaking elongation) was determined as 12 %. Tensile test results indicated that the highest weld efficiency was achieved with the specimen produced at the welding speed of 40 mm min^{-1}. The tensile strength of the welded specimens showed an average decrease of 38.3 % compared to the reference material. The welded joints usually fractured on the zones close to the weld centre.

Welding speed is an important parameter which affects the amount of heat generated in the FSW process [4]. During welding, the stirring zone (weld zone) is exposed to an intense amount of plastic deformation and high heat input. It is specified in the literature that this causes recrystallization at the stirring zone and dissolution and coarsening of the precipitation around the stirring zone [18, 19, 23]. The microstructural changes in these zones affect both the microstructure of the bond after welding and mechanical characteristics such as hardness and tensile strength [23]. When optimum welding parameters (rotational speed and welding speed) are used in FSW processes, welded joints with the most suitable mechanical properties can be achieved [18, 19]. However, it was assumed that the mechanical properties of specimens N1600-20 and N1600-40 were weakened by the zones on the weld metal which were not stirred homogeneously on the RS, and especially by the microscaled voids formed in the transition areas. Figure 8 shows the fracture form of specimen N1600-40. The tensile strength of the N1600-60 specimen was significantly reduced due to the holes that remained as a consequence of tunnel defects. The height of the tunnels increased, especially at high welding speeds, and resulted in such defects in the tensile specimen. Although the weld nugget exhibited fine grains and high
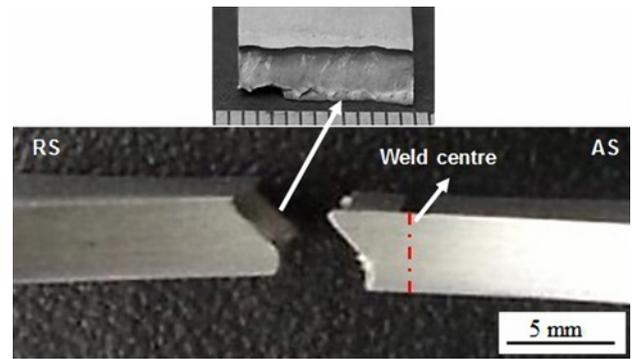
Fig. 8. Fracture form of specimen N1600-40.

hardness values, the defect on the weld root elicited a low mechanical response.

4. Conclusions

Plates of 7075 Al alloy were joined by FSW at 1600 rpm and welding speeds of 20, 40, and 60 mm min^{-1}. According to the data obtained as a result of mechanical and metallographic tests, the following conclusions may be stated:

1. Large grain bands with microvoid defects were formed on the retreating side of the weld nuggets.

2. The average grain size of the weld nuggets was reduced with an increase in welding speed.

3. No crack defects were observed in the weld nuggets. However, microvoid defects were formed, especially on the retreating side.

4. Welding speed affected the hardness distribution. A W-shaped hardness distribution pattern was detected in the weld zone of the specimens. In all specimens, the lowest hardness values were determined on the TMAZs.

5. The highest mechanical properties were obtained with the specimen produced at a welding speed of 40 mm min^{-1}. However, a decrease of 36 % in the tensile strength of this specimen was observed compared to the reference material.

6. The microvoid defects formed in the weld zones were attributed to the decrease in the tensile strength and % elongation values of the welded specimens.

Acknowledgements

References

[1] Ozyurek, D., Yilmaz, R., Kibar, E.: Journal of the Faculty of Engineering and Architecture of Gazi University, *27*, 2012, p. 193.

[2] Mahoney, M. W., Rhodes, C. G., Flintoff, J. G., Bingel, W. H., Spurling, R. A.: Metallurgical and Materials Transactions A, *29*, 1998, p. 1955. doi:10.1007/s11661-998-0021-5

[3] Rao, T. S., Reddy, G. M., Rao, G. S., Rao, S. R. K.: International Journal of Materials Research, *105*, 2014, p. 375. doi:10.3139/146.111033

[4] Kurt, A., Boz, M., Ozdemir, M.: Journal of the Faculty of Engineering and Architecture of Gazi University, *19*, 2004, p. 191.

[5] Rajakumar, S., Muralidharan, C., Balasubramanian, V.: Materials & Design, *32*, 2011, p. 535. doi:10.1016/j.matdes.2010.08.025

[6] Boz, M., Kurt, A.: Materials & Design, *25*, 2004, p. 343. doi:10.1016/j.matdes.2003.11.005

[7] Di, S., Yang, X., Fang, D., Luan, G.: Materials Chemistry and Physics, *104*, 2007, p. 244. doi:10.1016/j.matchemphys.2007.01.023

[8] Odabas, C.: Welding of Aluminium and Alloys. Istanbul, Askaynak 2007.

[9] Gemme, F., Verreman, Y., Dubourg, L, Wanjara, P.: Fatigue & Fracture of Engineering Materials & Structures, *34*, 2011, p. 877. doi:10.1111/j.1460-2695.2011.01580.x

[10] Akbarinia, S., Arefi, A., Shahbaznia, M.: International Journal on Recent Technologies in Mechanical and Electrical Engineering, *2*, 2015, p. 7.

[11] Adamowski, J., Gambaro, C., Lertora, E., Ponte, M., Szkodo, M.: Archives of Materials Science and Engineering, *28*, 2007, p. 453.

[12] Inada, K., Fujii, H., Ji, Y. S., Sun, Y. F., Morisada, Y.: Science and Technology of Welding and Joining, *15*, 2010, p. 131. doi:10.1179/136217109X12568132624244

[13] Adamowski, J., Szkodo, M.: Journal of Achievements in Materials and Manufacturing Engineering, *20*, 2007, p. 403.

[14] Uygur, I.: Archives of Metallurgy and Materials, *57*, 2012, p. 53. doi:10.2478/v10172-011-0152-3

[15] Kurt, A., Uygur, I., Ates, H.: Materials Science Forum, *534–536*, 2007, p. 789.

[16] Chouhan, D., Pal, S. K., Garg, S.: Journal of Engineering Research and Applications, *3*, 2013, p. 1972.

[17] Cavaliere, P., Campanile, G., Panella, F. W., Squillace, A.: Journal of Materials Processing Technology, *180*, 2006, p. 263. doi:10.1016/j.jmatprotec.2006.06.015

[18] Azimzadegan, T., Serajzadeh, S.: Journal of Materials Engineering and Performance, *19*, 2010, p. 1256. doi:10.1007/s11665-010-9625-1

[19] Rajakumar, S., Muralidharan, C., Balasubramanian, V.: Experimental Techniques, *36*, 2010, p. 1. doi:10.1111/j.1747-1567.2010.00677.x

[20] Yutaka, S. S., Kokawa, H.: Metallurgical and Materials Transactions A, *32*, 2001, p. 3023. doi:10.1007/s11661-001-0177-8

[21] Chen, H. B., Yan, K., Lin, T., Chen, S. B., Jiang, C. Y., Zhao, Y.: Materials Science and Engineering A, *433*, 2006, p. 64. doi:10.1016/j.msea.2006.06.056

[22] Scialpi, A., De Filippis, L. C. A., Cavaliere, P.: Materials & Design, *28*, 2007, p. 1124. doi:10.1016/j.matdes.2006.01.031

[23] Dalkilic, S.: Journal of Aeronautics and Space Technologies, *5*, 2012, p. 25.